Fluorescent H_2 Emission Lines from the Reflection Nebula NGC 7023 Observed with IGRINS

Present at Cosmic Cycle 2018 – ICISE QUY NHON

2018.07.12 by

Huynh Anh N. Le[1] and Soojong Pak[2] , and IGRINS team

[1]*Department of Physics and Astronomy, Seoul National University*

[2]*School of Space Research, Kyung Hee University*

Image from
http://www.cosmotography.com/images/lrg_ngc7023.html

IGRINS

(Immersion GRating INfrared Spectrograph)

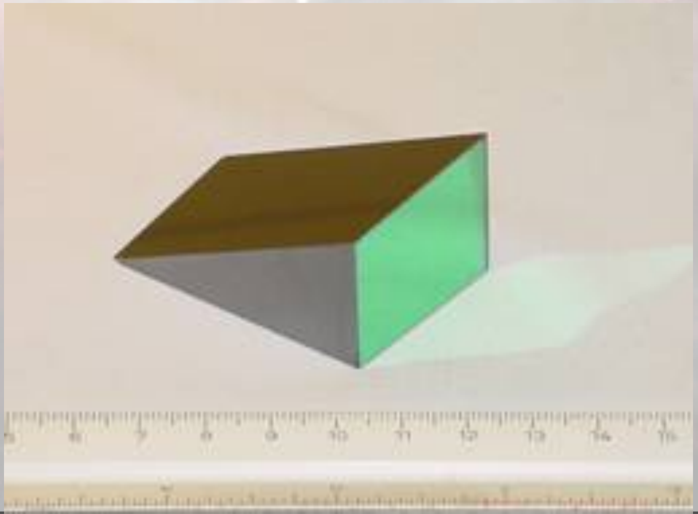

IGRINS Project (2010-2014)

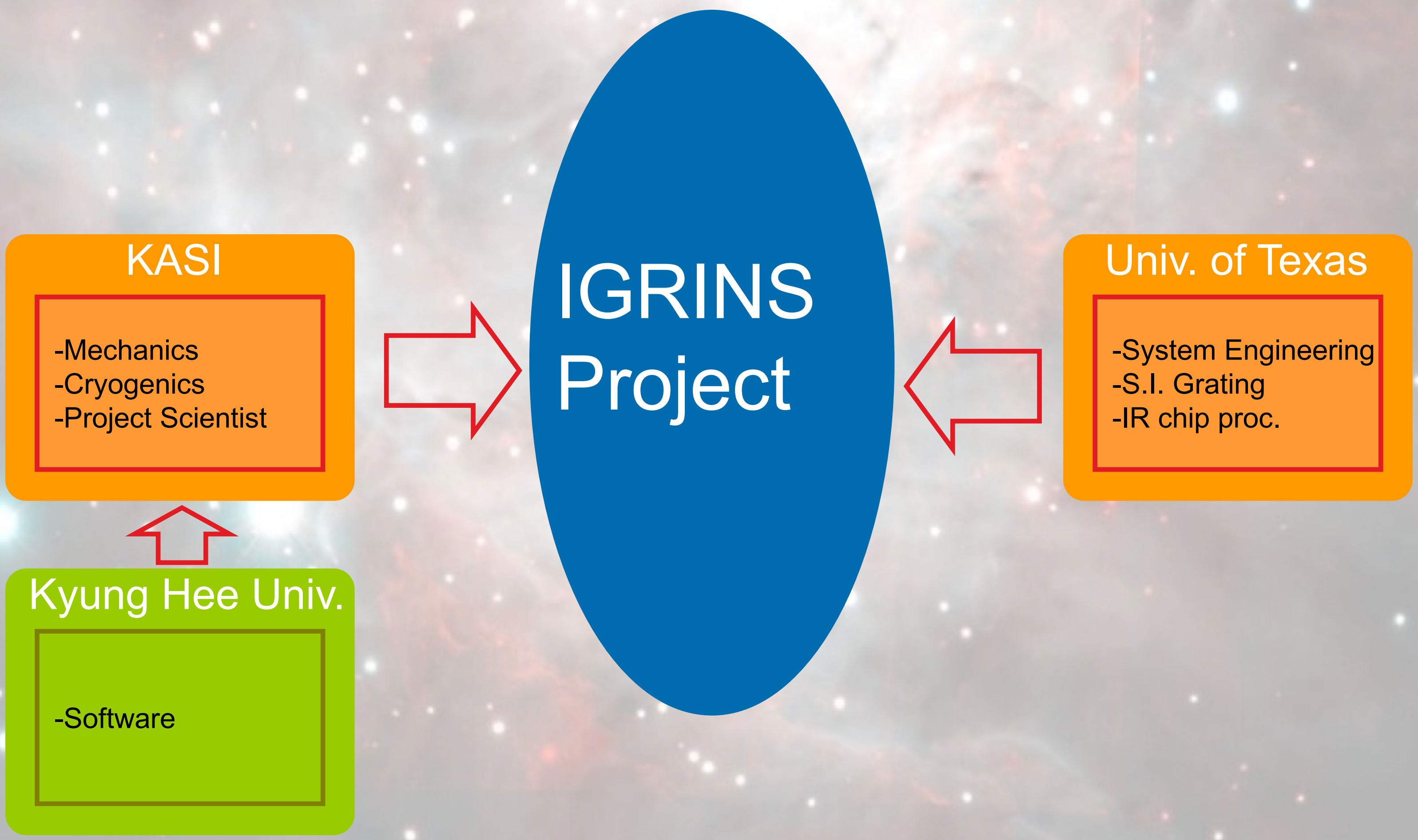

Concept of the Instrument

- IGRINS is a high resolution near-IR spectrograph
  - Simultaneous Dual Channel in H and K Bands
  - R= 45,000 (~7 km/s)
  - Slit 1”x 15”
  - no moving parts

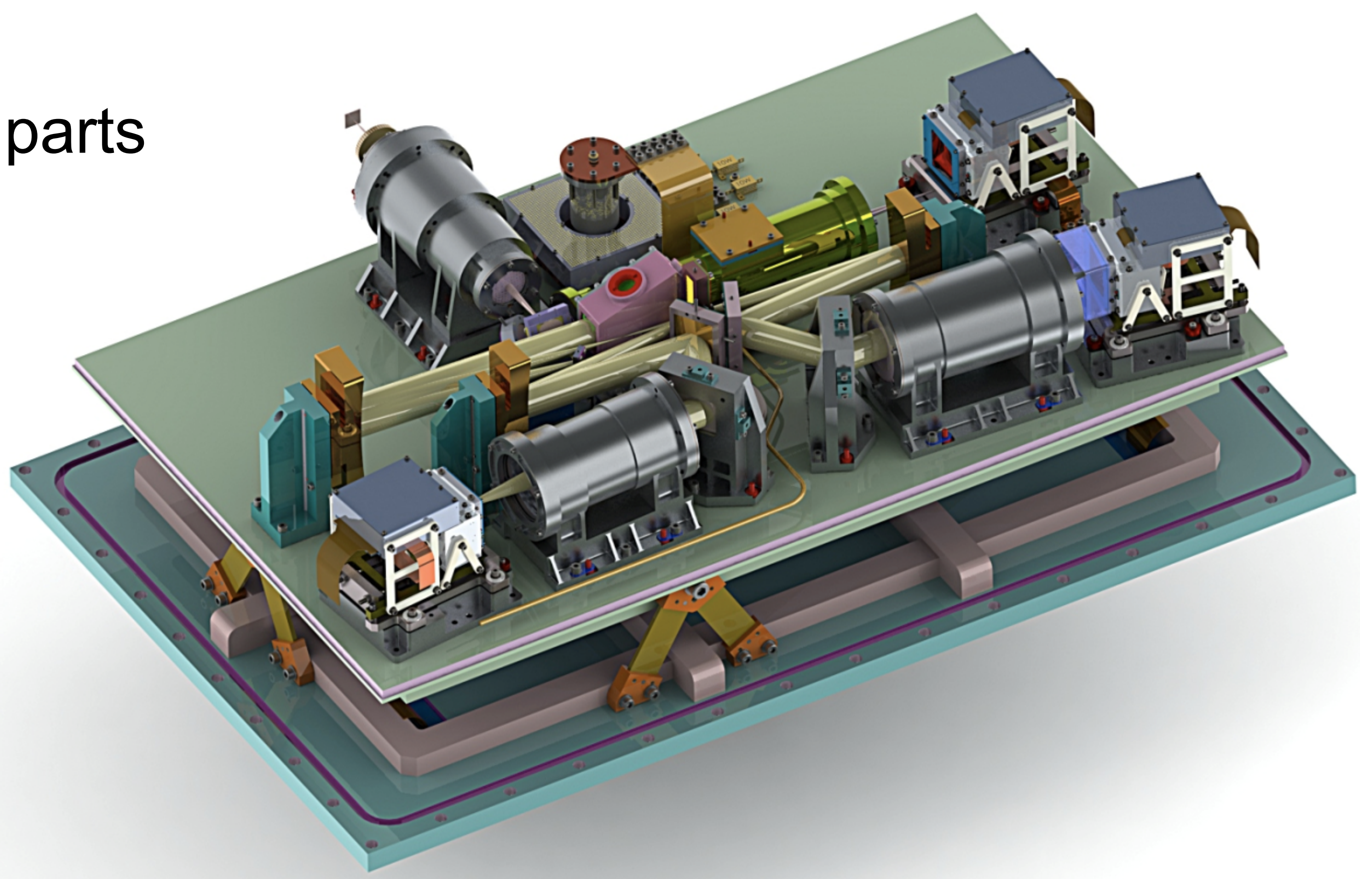

Design Layout

- Compatible with telescope diameters from 2.7m to 8m.
- H & K band covered by two separate cameras.
- White-pupil cross-dispersion.

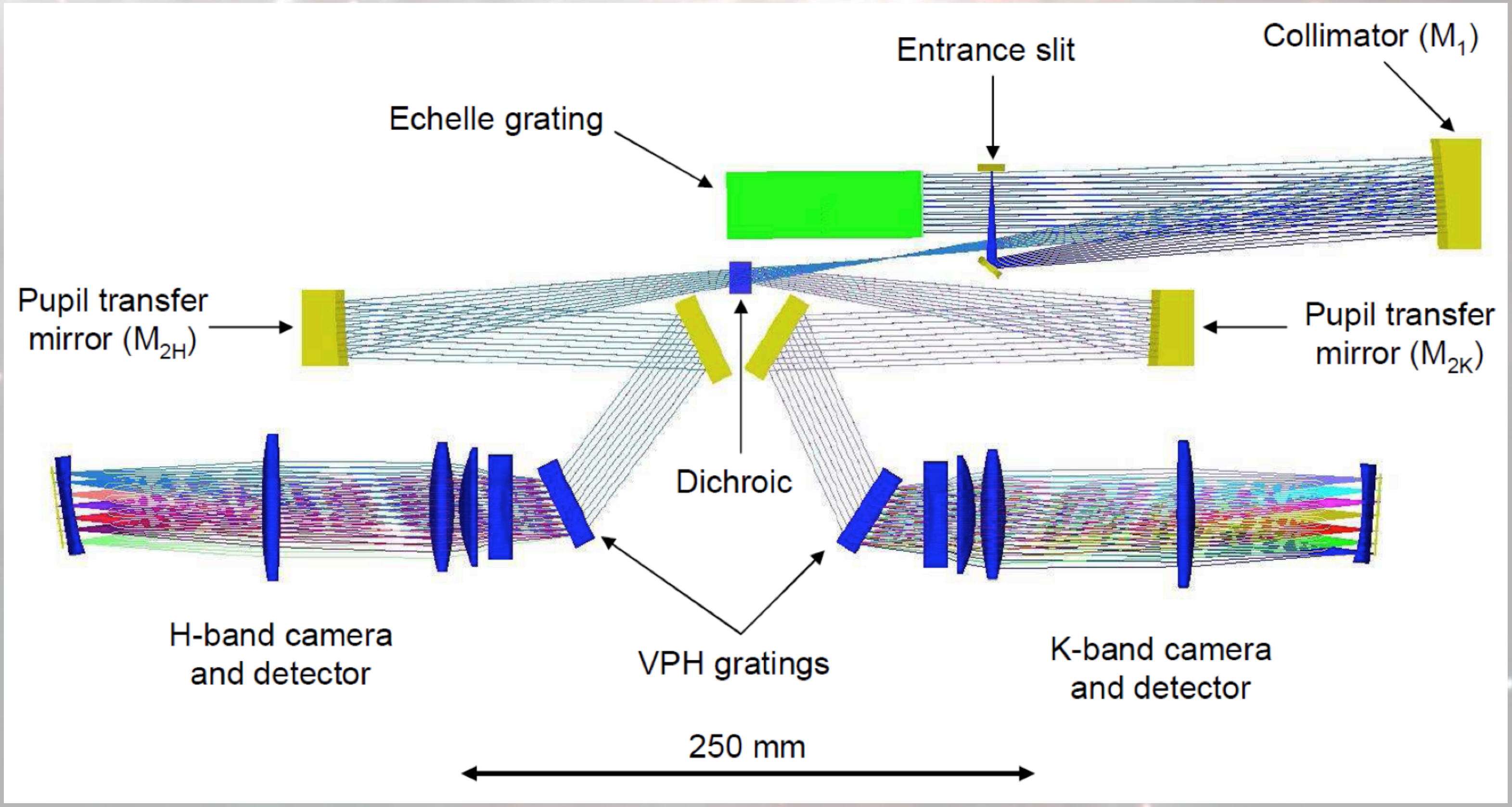

Prof. Daniel T. Jaffe

IGRINS Installation (2014 March)

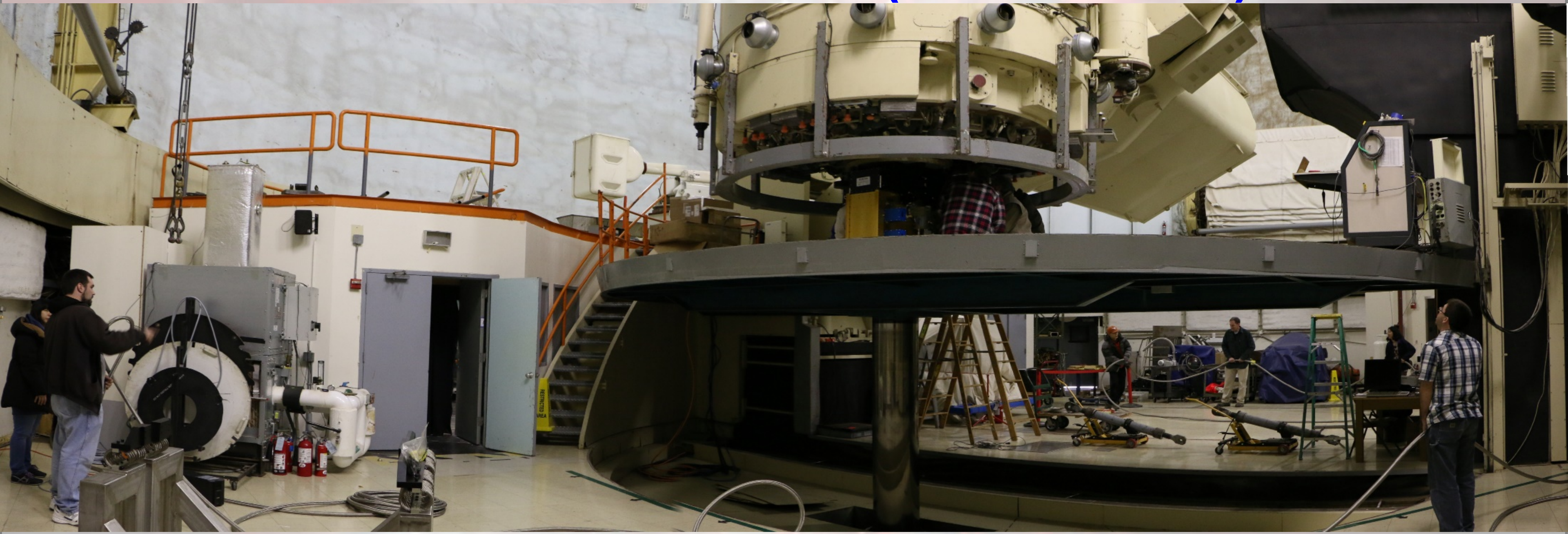

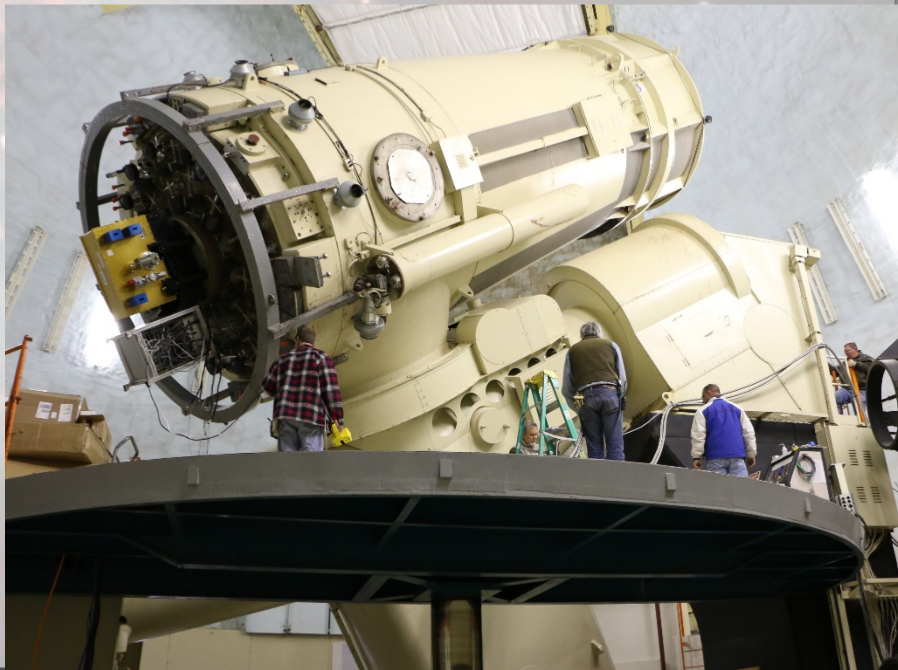

IGRINS on 2.7m Telescope (2014 March)

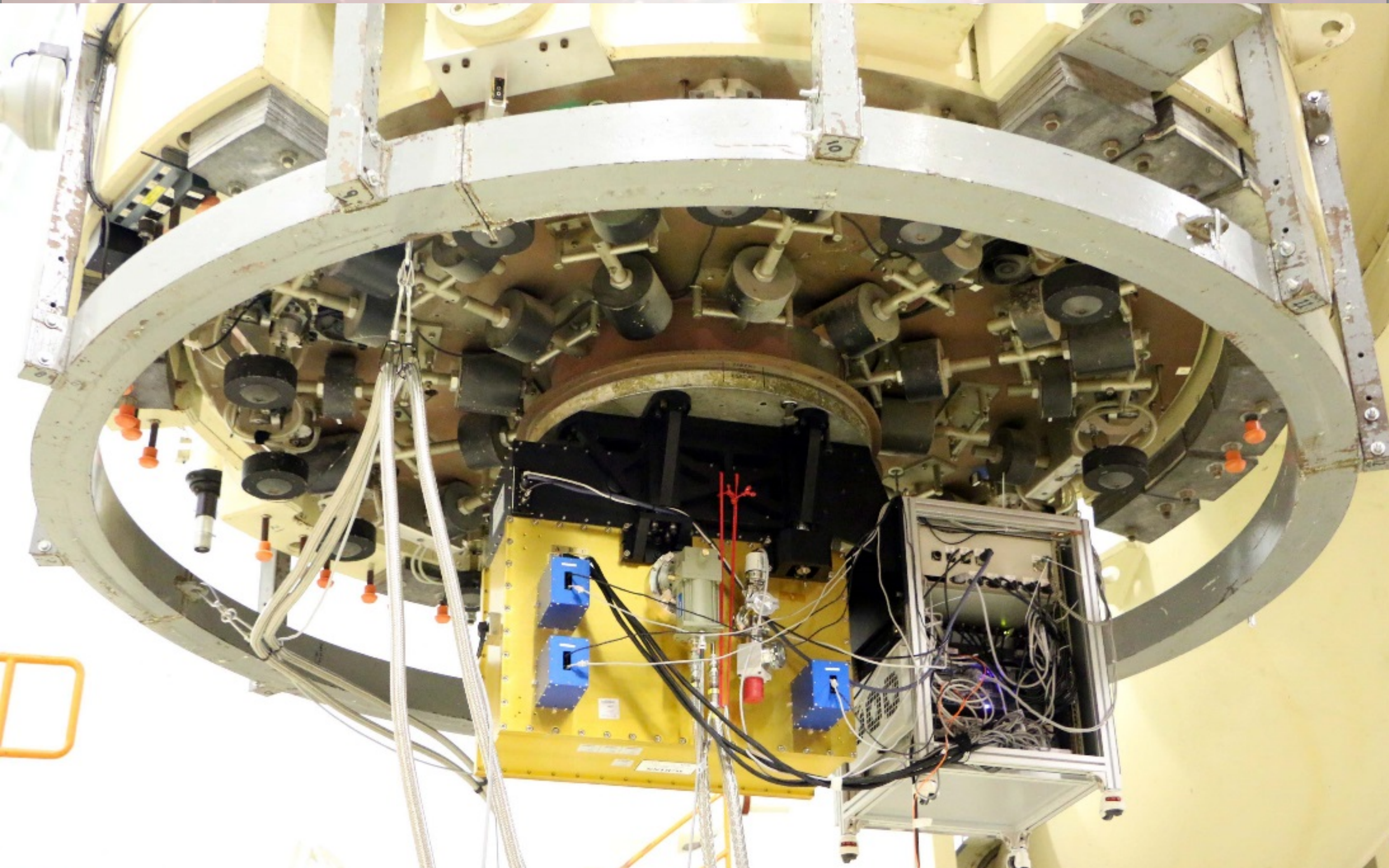

High Spectral Resolution Spectroscopy in Near-IR Bands

Advantages of High Spectral Spectroscopy in near-IR

- To isolate celestial lines from the crowded *telluric absorption* and emission lines.

  → Increasing S/N.

- To derive kinematics (~km/s).

Molecular Hydrogen Observations in Molecular Clouds

Iris

Horse head

Orion

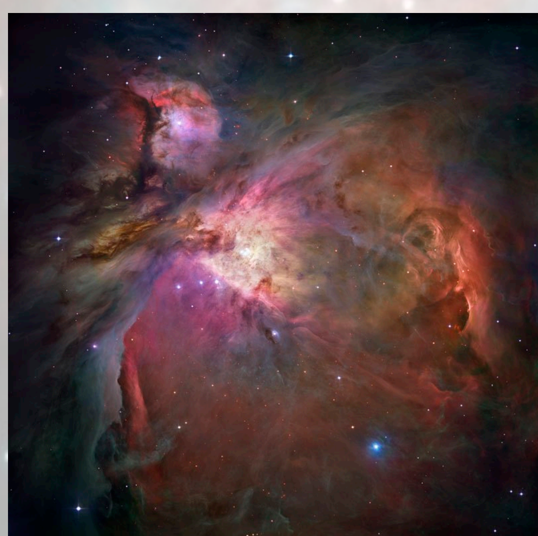

M1

Molecular Hydrogen

- The most abundant molecular
- Tracing ***interaction*** bet, the star and the cloud.
  - Shocked Region
  - Photodissociation Region

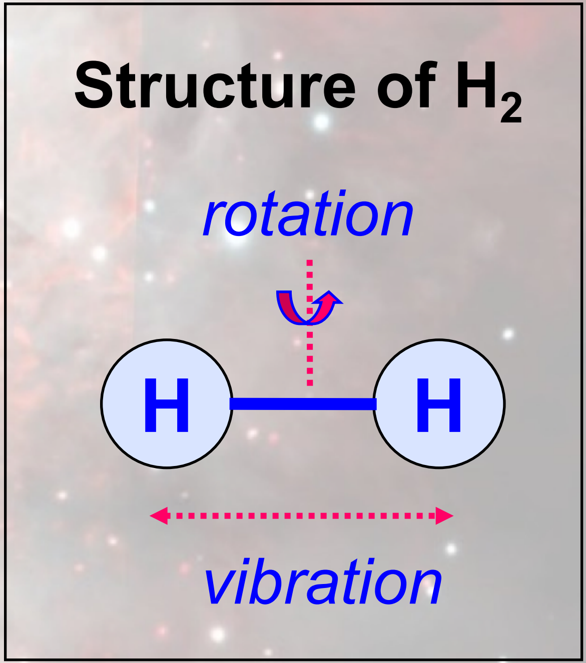

TABLE 1

Branch Notation

Branch	$J_{up} - J_{lo}$
O....................	−2
P	−1
Q....................	0
R....................	+1
S	+2

Shaw et al. (2005)

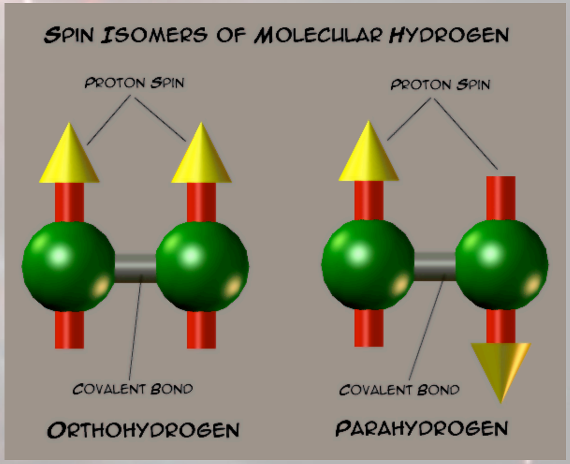

Thermal

Collisional Excitation
by shock
in IR bands

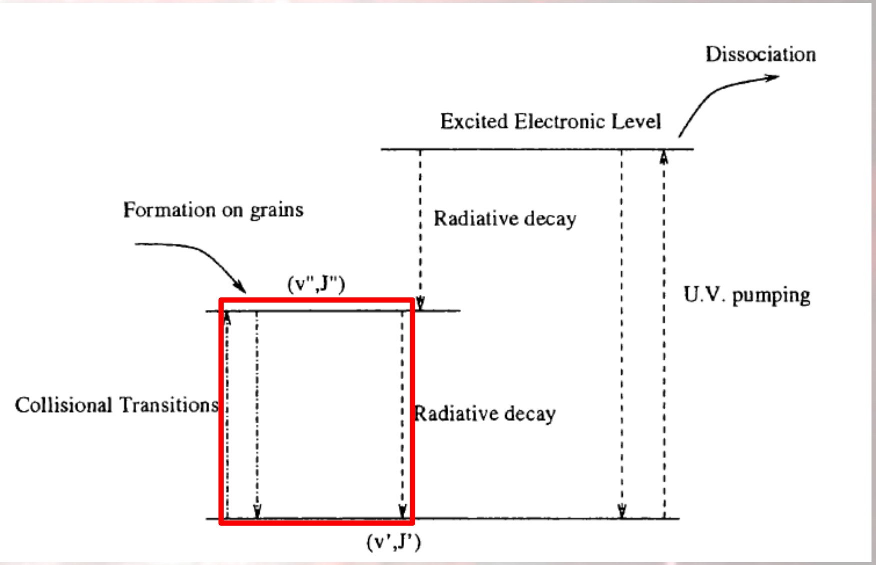

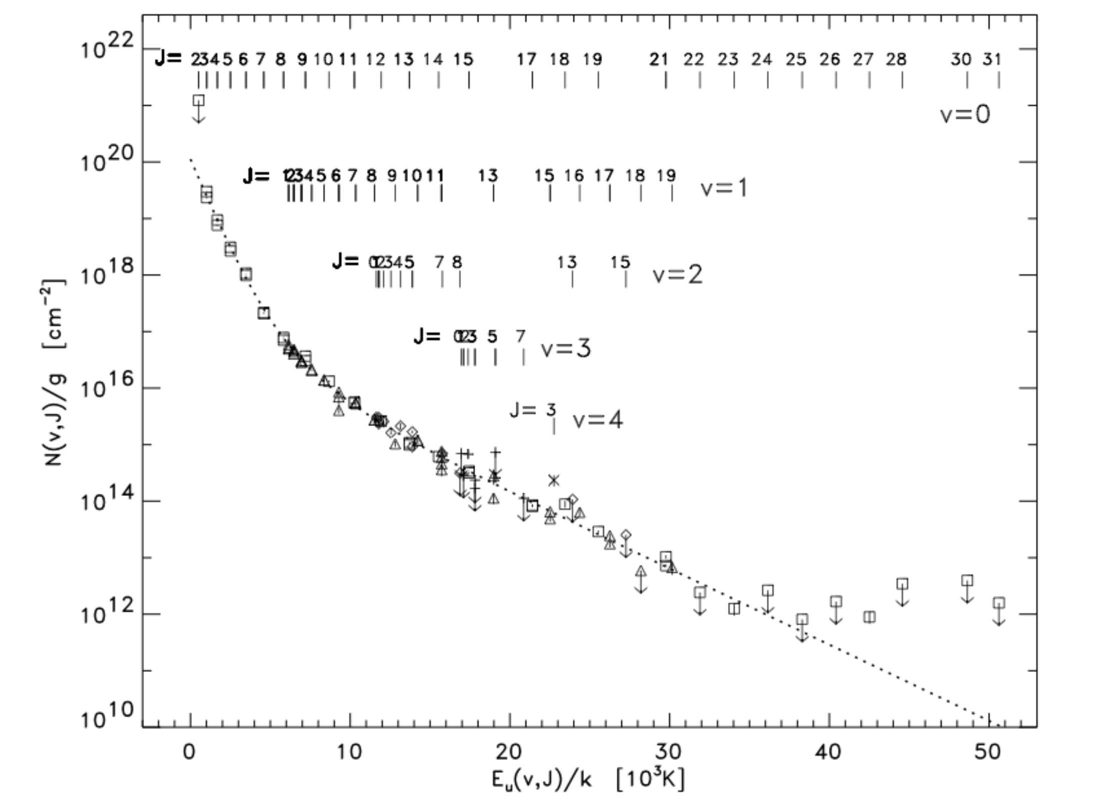

Rosenthal et al. (2000)

Non-Thermal

Electrically Excited
by Absorbing far-UV
and Radiates
in far-UV and IR bands

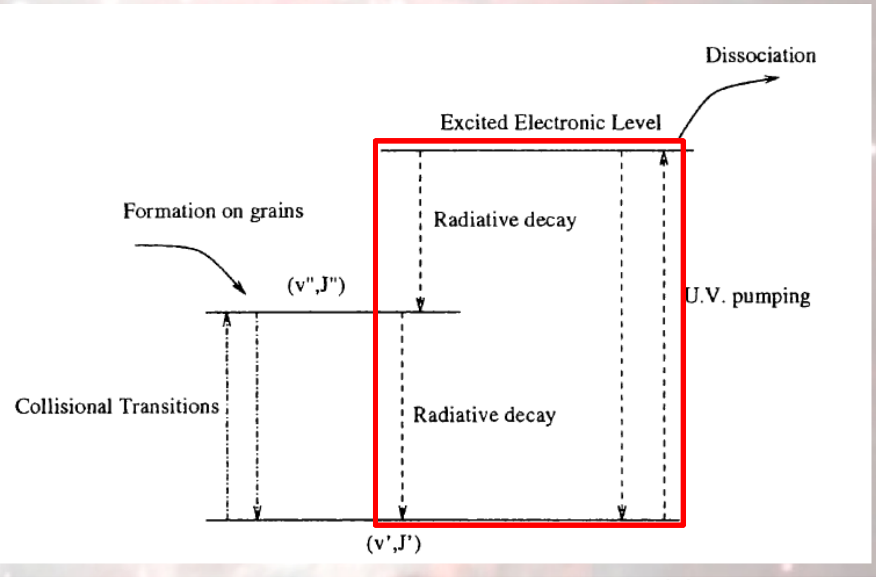

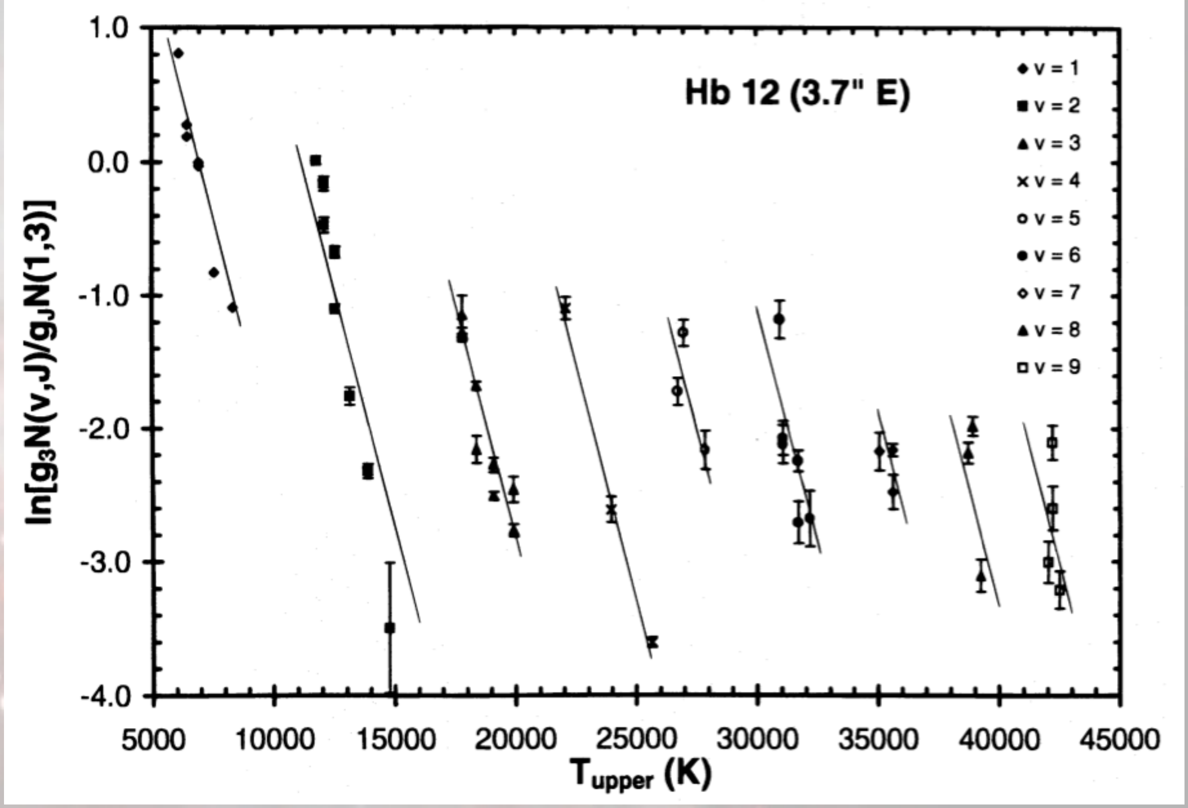

Hora & Latter (1996)

H_2 Excitation – Line Intensity & Ratio

Thermal by shocks	**Non-thermal** by Far-UV
Line ratio [2-1 S(1) / 1-0 S(1)]	
C-shocks : ~ 0.2 **J-shocks : < 0.5** **slow J-shocks (< 24 km/s): < 0.3**	**PDR (n_{H2} < 5 x 10^4 /cm^3): ~ 0.6** **dense PDR : < 0.6**

Measured ratio = 0.3 ~ 0.5

possible mechanism:

- pure dense PDR
- pure J-shocks, C+J-shocks
- PDR + shocks

Constellation: Cepheus

NGC 7023 (Iris Nebula)

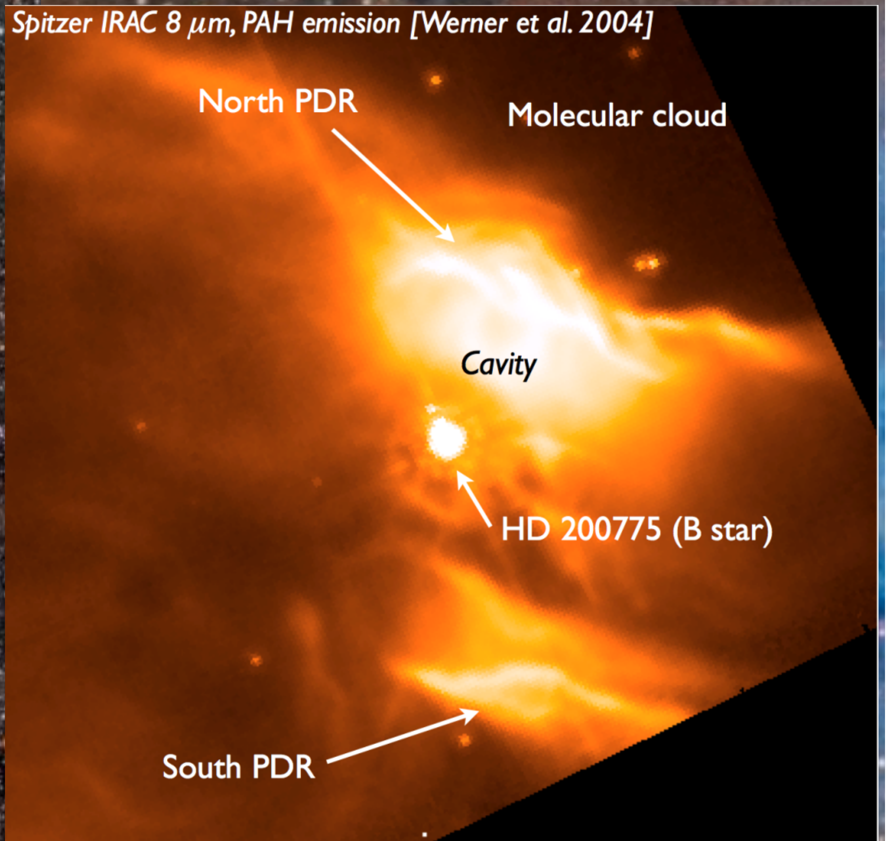

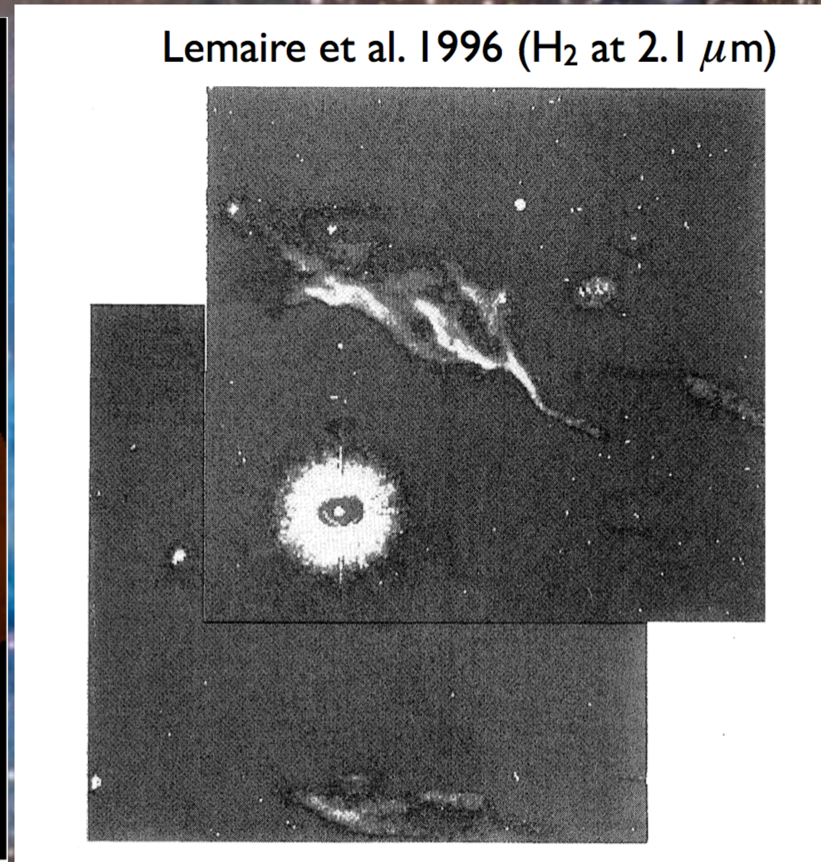

NGC 7023 (Iris Nebula)

- Illuminated by HD 200775 (Herbig B3Ve-B5, T_{eff} = 17,000 K)
- PDRs in North and South from HD 200775
- D = 430 (+160/-90) pc
- Clumpy structure ? (Martini+1999;1997)
- Advancing PDR ? (Fuente +2000)
- Existing of shock ? (Fuente +2000)

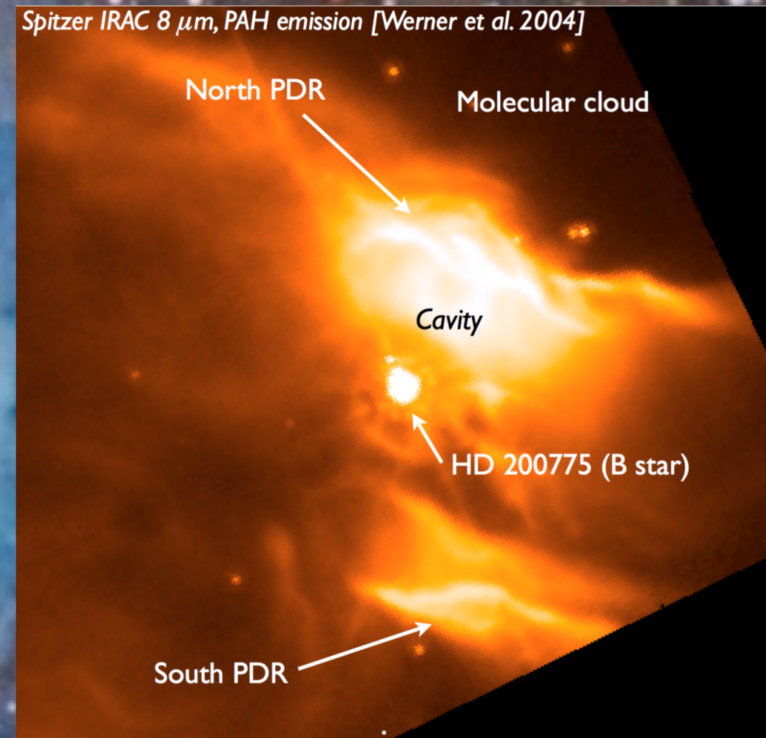

Spitzer IRAC 8 μm, PAH emission [Werner et al. 2004]

IGRINS - observations

- Target: NGC 7023
- Date: 2014 July 12 (Commissioning)
- Exposures: 2 x 600s / frame
- Positions (Ra, Dec)$_{J2000}$ = (21:01:36.9, +68:09:47.8)
- Total exposure time:

  t = 1200 s, ON position   t = 1200 s, OFF position

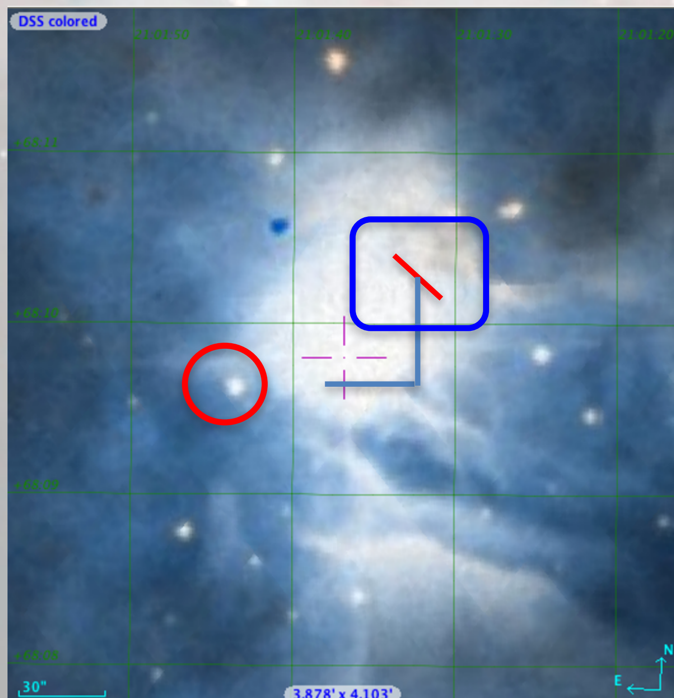

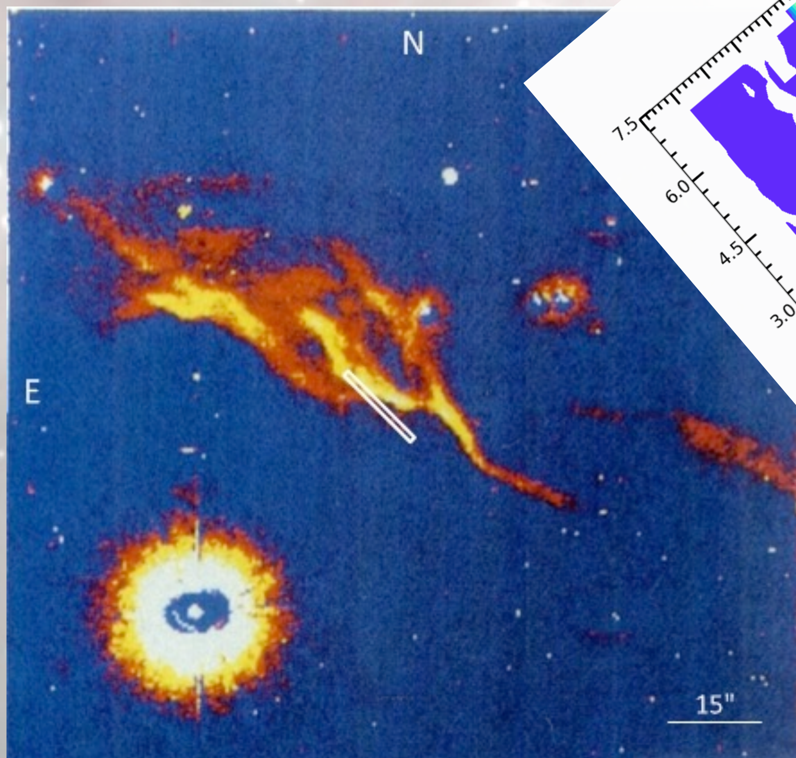

Lemaire et al. (1996)

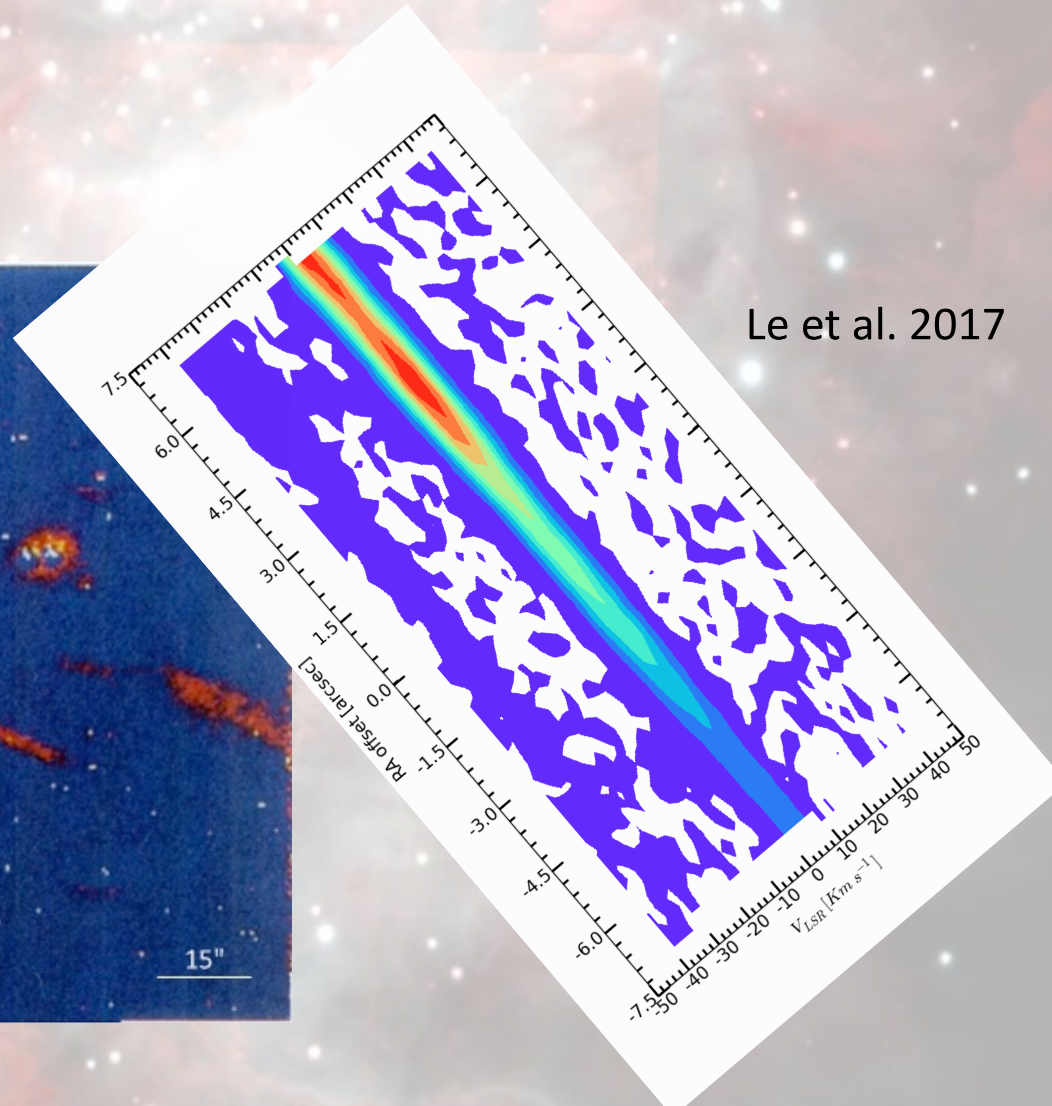

Le et al. 2017

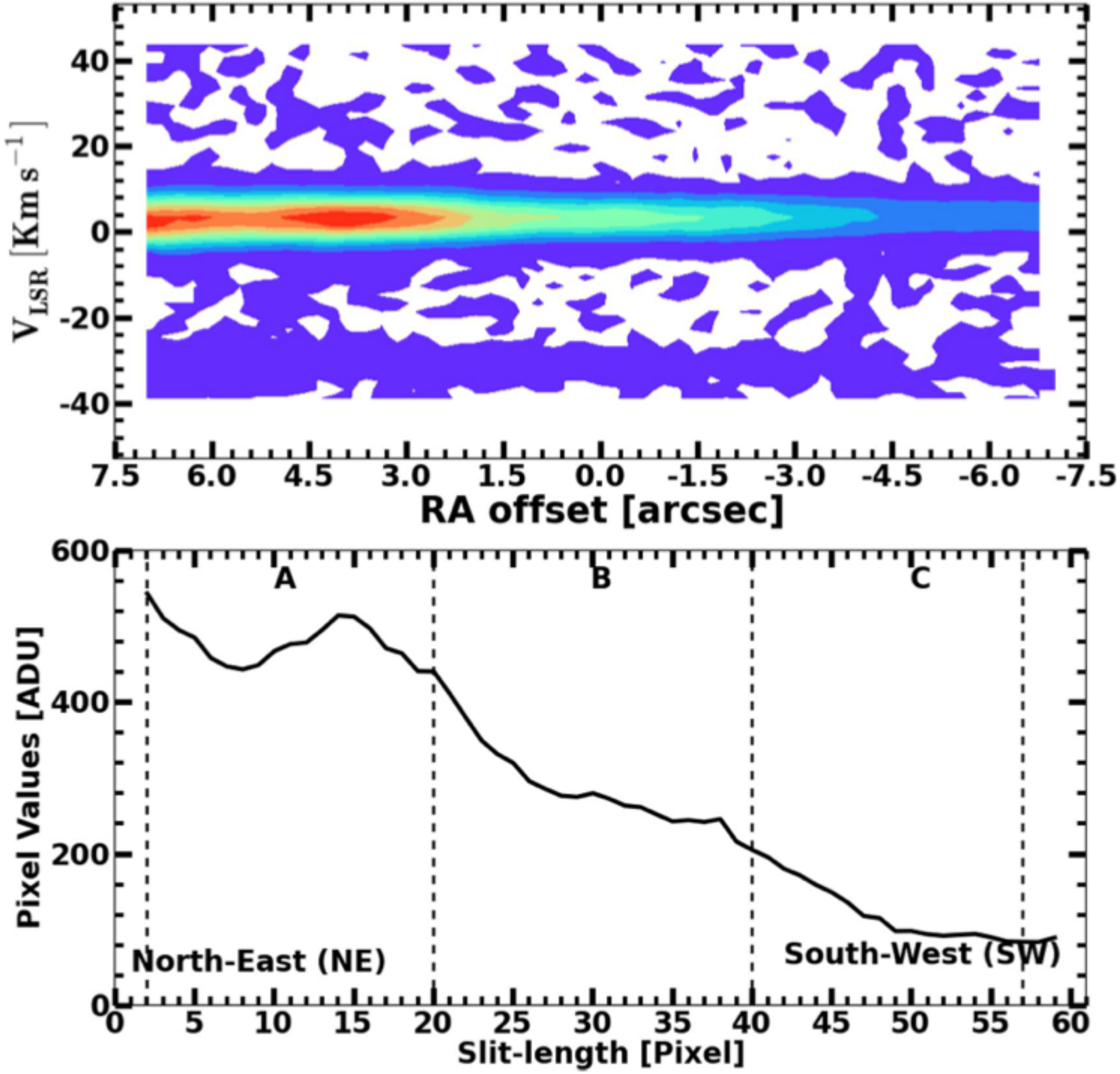

Figure 4. Radial velocity diagram of the 1-0 S(1) line (top plot). In the diagram, $1'' = 3.66$ pixels. The bottom plot shows the intensity profile at the peak of the 1-0 S(1) line. The black dashed lines show the separated regions A, B, and C along the slit length.

H_2 spectra

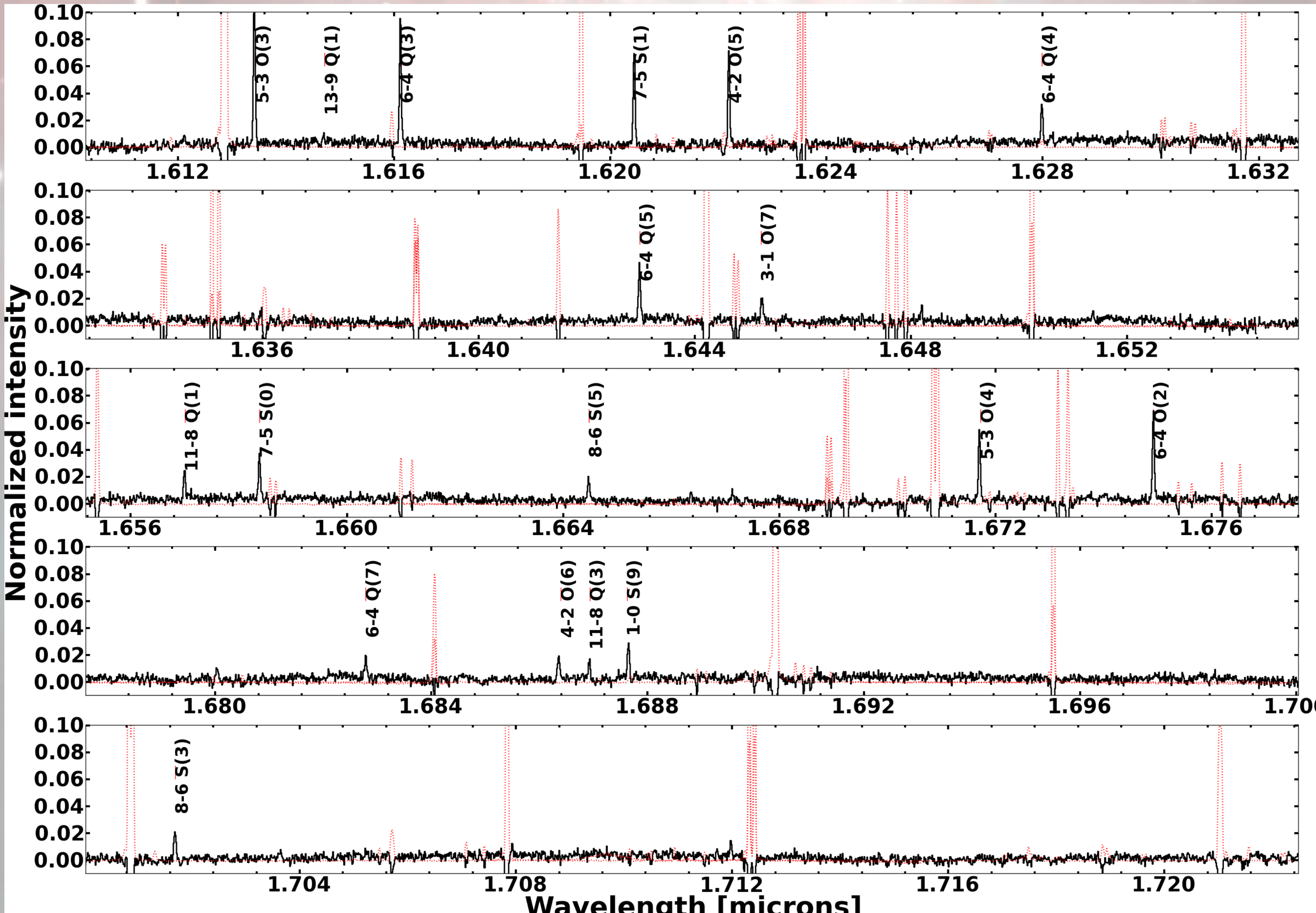

Normalized intensity
Wavelength [microns]
5-3 O(3)
13-9 Q(1)
6-4 Q(3)
7-5 S(1)
4-2 O(5)
6-4 Q(4)
6-4 Q(5)
3-1 O(7)
11-8 Q(1)
7-5 S(0)
8-6 S(5)
5-3 O(4)
6-4 O(2)
6-4 Q(7)
4-2 O(6)
11-8 Q(3)
1-0 S(9)
8-6 S(3)

H_2 spectra

- 68 H_2 rovibrational emission lines (v = 1 – 13 and J = 1 – 11) from Regions A, B, and C

Table 1
NGC 7023 H_2 Line Observation

Line	λ^a	Region A			Region B			Region C		
		I^b	I^c	$\ln(N_u/g)^d$	I^b	I^c	$\ln(N_u/g)^d$	I^b	I^c	$\ln(N_u/g)^d$
4-2 Q(9)	1.498884	0.863(0.107)	0.041(0.005)	27.867(0.124)	···	···	···	···	···	···
4-2 O(3)	1.509865	5.782(0.311)	0.275(0.015)	31.156(0.054)	4.432(0.269)	0.372(0.024)	30.890(0.061)	2.731(0.224)	0.511(0.044)	30.406(0.082)
5-3 Q(4)	1.515792	2.356(0.229)	0.112(0.011)	30.306(0.097)	1.737(0.168)	0.146(0.014)	30.001(0.096)	···	···	···
3-1 O(5)	1.522026	2.920(0.188)	0.139(0.009)	30.990(0.064)	2.271(0.172)	0.190(0.015)	30.739(0.076)	2.022(0.212)	0.378(0.041)	30.623(0.105)
5-3 Q(5)	1.528641	2.562(0.199)	0.122(0.010)	29.125(0.078)	2.251(0.186)	0.189(0.016)	28.996(0.083)	1.320(0.131)	0.247(0.025)	28.462(0.099)
6-4 S(0)	1.536908	1.942(0.150)	0.092(0.007)	30.600(0.077)	2.134(0.156)	0.179(0.013)	30.694(0.073)	···	···	···
10-7 O(3)	1.548851	1.039(0.111)	0.049(0.005)	29.146(0.106)	0.893(0.102)	0.075(0.009)	28.995(0.114)	0.488(0.072)	0.091(0.014)	28.390(0.148)
5-3 O(2)	1.560730	2.524(0.169)	0.120(0.008)	31.481(0.067)	1.876(0.138)	0.157(0.012)	31.184(0.073)	1.113(0.114)	0.208(0.022)	30.662(0.103)
5-3 Q(7)	1.562627	1.578(0.120)	0.075(0.006)	28.402(0.076)	1.285(0.098)	0.108(0.008)	28.196(0.076)	···	···	···
4-2 O(4)	1.563516	2.546(0.160)	0.121(0.008)	31.355(0.063)	2.340(0.139)	0.196(0.012)	31.271(0.059)	1.311(0.110)	0.245(0.022)	30.692(0.084)
7-5 S(2)	1.588290	1.240(0.113)	0.059(0.005)	29.124(0.091)	0.973(0.097)	0.082(0.008)	28.881(0.100)	0.860(···)	0.161(···)	28.758(···)
6-4 Q(1)	1.601535	3.992(0.193)	0.190(0.010)	30.248(0.048)	3.369(0.173)	0.283(0.015)	30.078(0.051)	2.222(0.134)	0.416(0.028)	29.662(0.060)
6-4 Q(2)	1.607386	3.813(0.194)	0.182(0.010)	31.136(0.051)	2.255(0.157)	0.189(0.014)	30.611(0.070)	1.600(0.138)	0.299(0.027)	30.268(0.086)
5-3 O(3)	1.613536	4.932(0.237)	0.235(0.012)	30.697(0.048)	4.112(0.214)	0.345(0.019)	30.515(0.052)	2.549(0.165)	0.477(0.034)	30.037(0.065)
13-9 Q(1)	1.614812	0.247(0.057)	0.012(0.003)	28.383(0.233)	···	···	···	···	···	···
6-4 Q(3)	1.616211	2.879(0.158)	0.137(0.008)	29.505(0.055)	2.353(0.136)	0.197(0.012)	29.303(0.058)	1.673(0.116)	0.313(0.023)	28.963(0.069)
7-5 S(1)	1.620530	2.723(0.145)	0.130(0.007)	29.208(0.053)	2.283(0.143)	0.191(0.013)	29.032(0.063)	1.098(0.116)	0.205(0.022)	28.300(0.106)
4-2 O(5)	1.622292	3.133(0.162)	0.149(0.008)	30.507(0.052)	2.716(0.154)	0.228(0.014)	30.364(0.057)	1.914(0.143)	0.358(0.029)	30.014(0.075)
6-4 Q(4)	1.628084	0.982(0.098)	0.047(0.005)	29.325(0.100)	0.718(0.093)	0.060(0.008)	29.012(0.129)	0.492(0.074)	0.092(0.014)	28.634(0.151)
6-4 Q(5)	1.643080	1.858(0.129)	0.088(0.006)	28.703(0.070)	1.425(0.115)	0.119(0.010)	28.438(0.081)	0.832(0.084)	0.156(0.016)	27.900(0.101)
3-1 O(7)	1.645324	0.668(0.068)	0.032(0.003)	29.871(0.102)	0.615(0.065)	0.052(0.006)	29.789(0.106)	0.353(0.051)	0.066(0.010)	29.233(0.145)
11-8 Q(1)	1.657105	0.730(0.083)	0.035(0.004)	28.851(0.114)	0.570(0.075)	0.048(0.006)	28.604(0.131)	0.545(0.066)	0.102(0.013)	28.558(0.122)
7-5 S(0)	1.658482	1.054(0.087)	0.050(0.004)	30.020(0.083)	0.818(0.095)	0.069(0.008)	29.767(0.116)	···	···	···
8-6 S(5)	1.664578	0.518(0.075)	0.025(0.004)	26.994(0.144)	···	···	···	···	···	···
5-3 O(4)	1.671821	1.999(0.138)	0.095(0.007)	30.793(0.069)	1.372(0.114)	0.115(0.010)	30.417(0.083)	1.382(0.107)	0.259(0.021)	30.424(0.077)
6-4 O(2)	1.675019	2.127(0.128)	0.101(0.006)	31.167(0.060)	1.451(0.102)	0.122(0.009)	30.784(0.071)	1.125(···)	0.211(···)	30.530(···)
4-2 O(6)	1.686494	0.791(0.085)	0.038(0.004)	30.350(0.108)	···	···	···	···	···	···
1-0 S(9)	1.687721	1.017(0.108)	0.048(0.005)	29.014(0.106)	0.610(0.081)	0.051(0.007)	28.504(0.133)	0.205(0.045)	0.038(0.008)	27.415(0.218)
8-6 S(3)	1.701797	1.005(0.099)	0.048(0.005)	27.806(0.098)	0.846(0.093)	0.071(0.008)	27.635(0.110)	0.453(0.068)	0.085(0.013)	27.010(0.150)
7-5 Q(1)	1.728779	3.613(0.211)	0.172(0.010)	30.150(0.058)	2.836(0.207)	0.238(0.018)	29.907(0.073)	2.394(0.129)	0.448(0.027)	29.738(0.054)
6-4 O(3)	1.732637	4.227(0.233)	0.201(0.011)	30.382(0.055)	3.519(0.212)	0.295(0.019)	30.199(0.060)	1.776(0.129)	0.332(0.026)	29.515(0.073)
5-3 O(5)	1.735888	3.222(0.159)	0.153(0.008)	30.194(0.049)	2.298(0.154)	0.193(0.013)	29.856(0.067)	···	···	···
1-0 S(7)	1.748035	3.624(0.218)	0.173(0.011)	29.937(0.060)	2.475(0.204)	0.208(0.018)	29.555(0.082)	···	···	···
4-2 O(7)	1.756296	0.873(0.091)	0.042(0.004)	29.527(0.105)	0.645(0.070)	0.054(0.006)	29.225(0.108)	0.351(0.052)	0.066(0.010)	28.617(0.148)
11-8 O(3)	1.760929	0.940(0.100)	0.045(0.005)	29.124(0.106)	···	···	···	···	···	···
7-5 O(5)	2.022040	1.022(0.078)	0.049(0.004)	28.774(0.076)	0.972(0.073)	0.082(0.006)	28.724(0.075)	0.247(0.031)	0.046(0.006)	27.356(0.124)
6-4 O(7)	2.029694	0.415(0.043)	0.020(0.002)	28.161(0.104)	···	···	···	···	···	···
1-0 S(2)	2.033756	9.052(0.224)	0.431(0.012)	32.560(0.025)	5.579(0.174)	0.468(0.017)	32.076(0.031)	2.795(0.118)	0.523(0.026)	31.385(0.042)
8-6 O(3)	2.041816	1.613(0.113)	0.077(0.005)	29.450(0.070)	1.436(0.103)	0.120(0.009)	29.333(0.072)	0.835(0.077)	0.156(0.015)	28.790(0.093)
3-2 S(5)	2.065557	1.335(0.096)	0.064(0.005)	28.924(0.072)	0.971(0.078)	0.081(0.007)	28.606(0.081)	0.518(0.049)	0.097(0.010)	27.978(0.095)
12-9 O(3)	2.069969	0.311(0.037)	0.015(0.002)	28.392(0.118)	0.289(0.035)	0.024(0.003)	28.321(0.122)	···	···	···
2-1 S(3)	2.073510	7.288(0.179)	0.347(0.010)	30.693(0.025)	4.718(0.141)	0.396(0.014)	30.258(0.030)	2.258(0.109)	0.423(0.023)	29.521(0.048)
9-7 Q(3)	2.100659	0.387(0.034)	0.018(0.002)	27.915(0.088)	···	···	···	···	···	···
8-6 O(4)	2.121570	0.610(0.044)	0.029(0.002)	29.429(0.072)	0.540(0.045)	0.045(0.004)	29.307(0.083)	0.220(0.025)	0.041(0.005)	28.409(0.114)
1-0 S(1)	2.121831	21.002(0.291)	1.000	32.734(0.014)	11.924(0.219)	1.000	32.168(0.018)	5.343(0.146)	1.000	31.366(0.027)
2-1 S(2)	2.154225	4.197(0.137)	0.200(0.007)	31.509(0.033)	2.683(0.114)	0.225(0.010)	31.061(0.043)	1.388(0.081)	0.260(0.017)	30.402(0.058)
9-7 O(2)	2.172704	0.317(0.035)	0.015(0.002)	29.556(0.109)	0.341(0.032)	0.029(0.003)	29.627(0.095)	0.079(0.012)	0.015(0.002)	28.169(0.156)

Analysis

- Dynamical Information from H_2 Lines
- Emission line ratios
- Ortho-to-para ratios
- H_2 level population

De-convolution of Line Width

	V	ΔV_{FWHM}
Region A	3.64 ± 0.16	4.63 ± 0.34
Region B	3.46 ± 0.11	3.29 ± 0.26
Region C	3.39 ± 0.22	3.20 ± 0.27

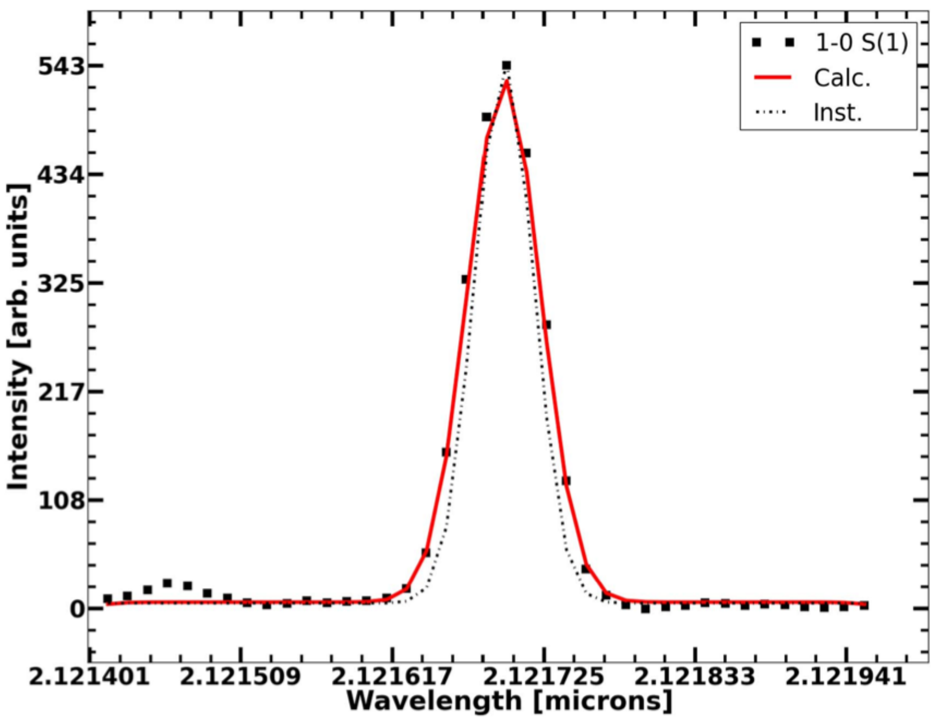

Figure 5. Observed H_2 1-0 S(1) line profile from region A in black squares. The black dotted points present the instrument profile. The solid red line is from the convolution of the instrument profile and the derived intrinsic line width.

Sample Spectra: H_2 1-0 S(1)

Line Analysis

	2-1 S(1) / 1-0 S(1)	Ortho-to-Para Ratio (OPR)
Region A	0.41 ± 0.01	1.82 ± 0.11
Region B	0.48 ± 0.02	1.75 ± 0.09
Region C	0.56 ± 0.03	1.63 ± 0.12

Exc. Diag. of H_2 level Column Density: ***Region A***

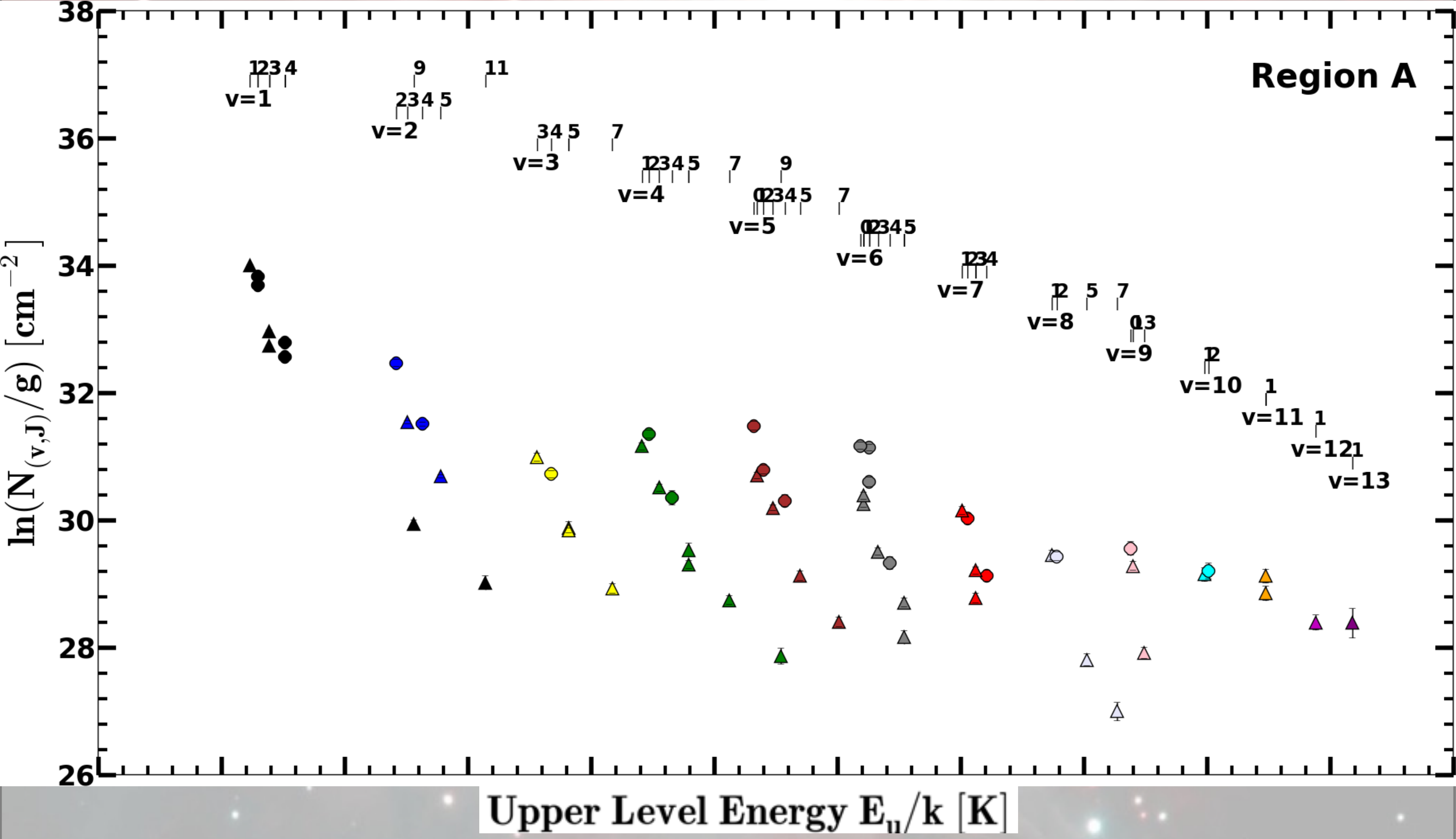

Exc. Diag. of H_2 level Column Density: ***Region B***

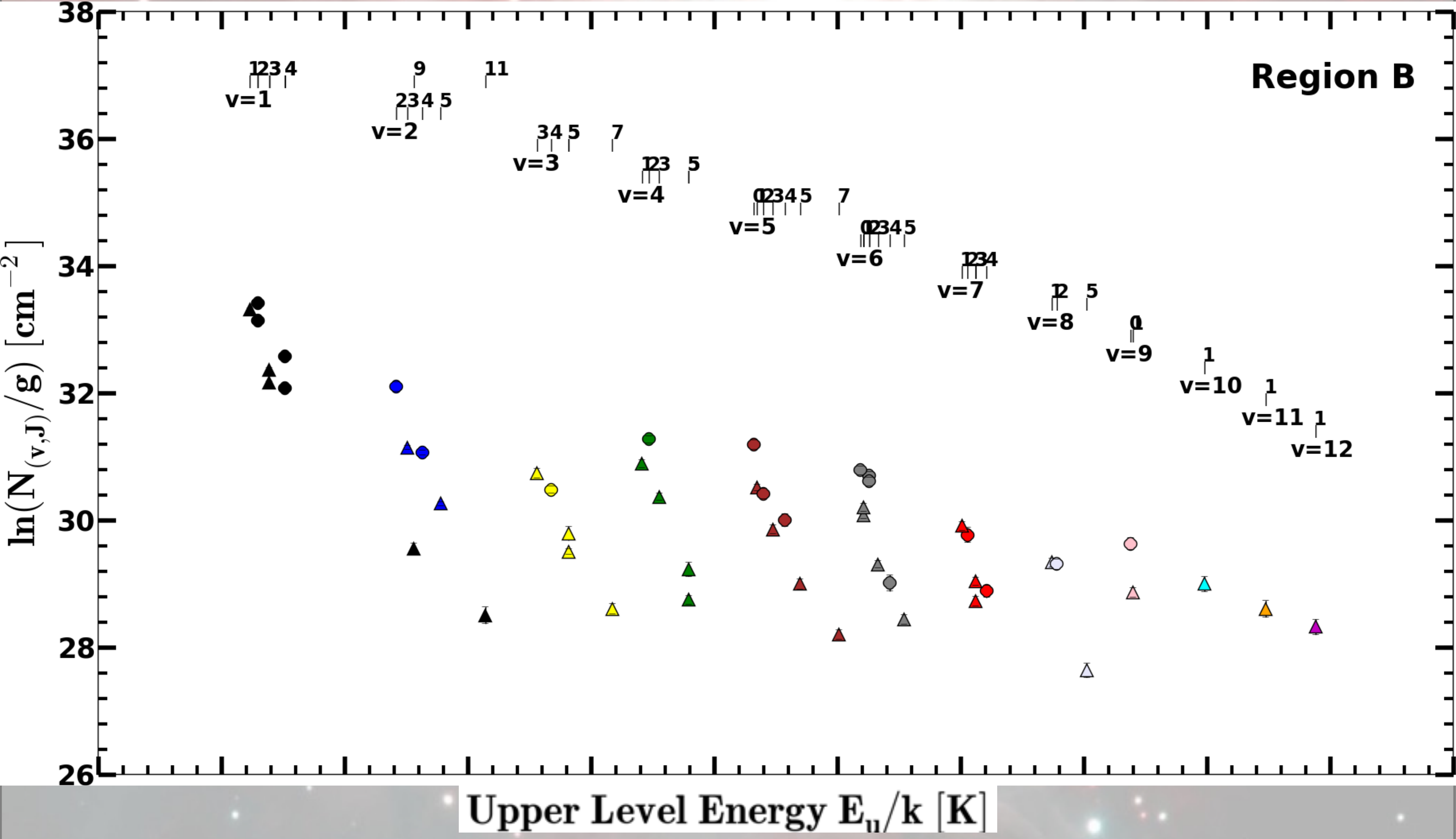

Exc. Diag. of H_2 level Column Density: ***Region C***

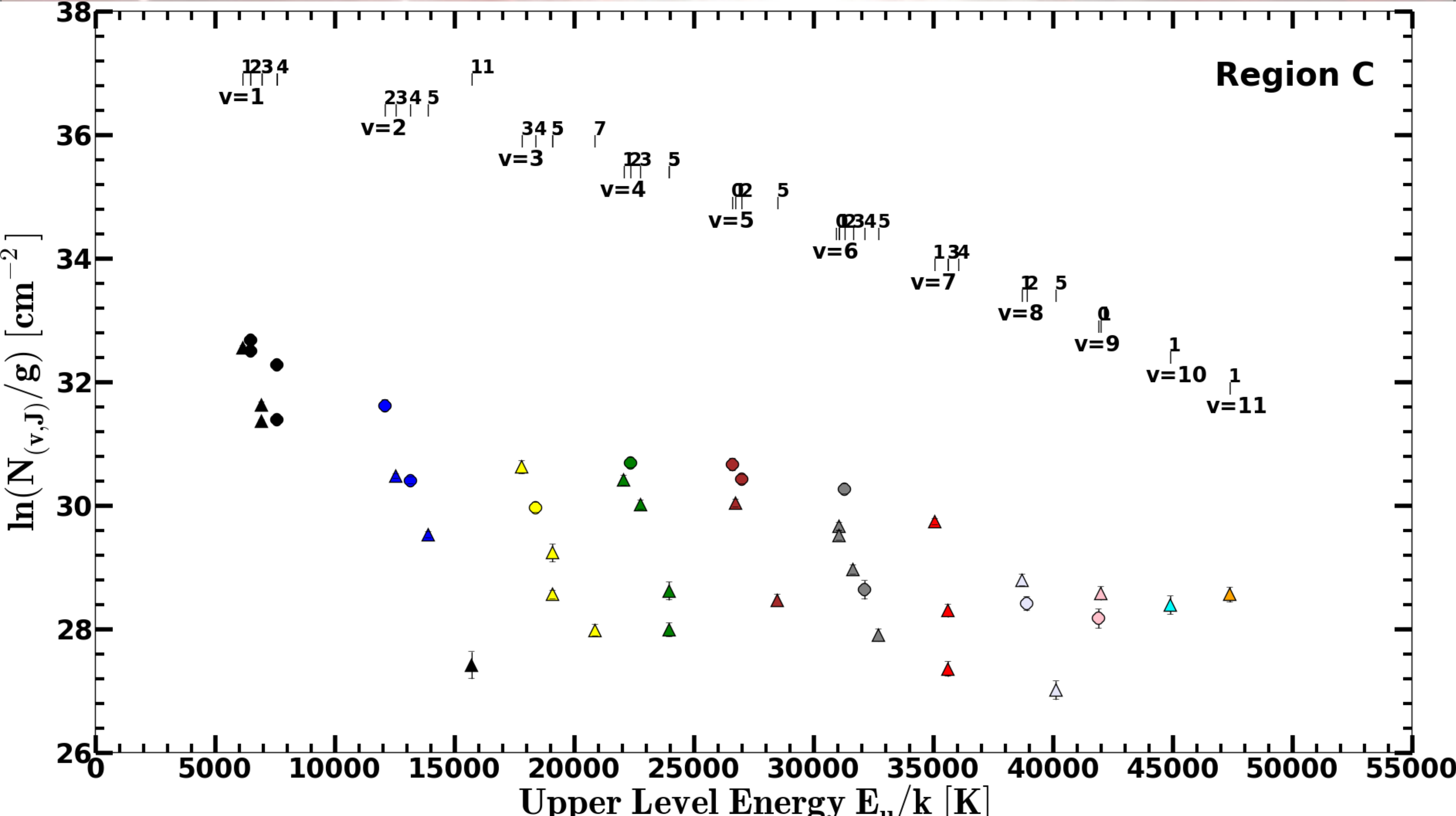

Comparison Data to PDR Model

Table 4
Gas Density from Comparison of the Line Ratios with the PDR Model of Draine & Bertoldi (1996)

Model	n_H (cm^{-3})	UV field strength [Habing]	χ^{2a}	χ^{2b}	χ^{2c}
aw3o	10^2	1	77	23	29
bw3d	10^2	10	91	26	31
Bw3o	10^3	10	86	25	30
Cw3o	10^3	10^2	52	16	26
Gw3o	10^4	10^2	25	15	26
Hw3o	10^4	10^3	26	17	27
Lw3o	10^5	10^3	32	38	39
Mw3o	10^5	10^4	57	53	48
Qw3o	10^6	10^4	75	85	63

Notes.
[a] χ^2 of region A.
[b] χ^2 of region B.
[c] χ^2 of region C.

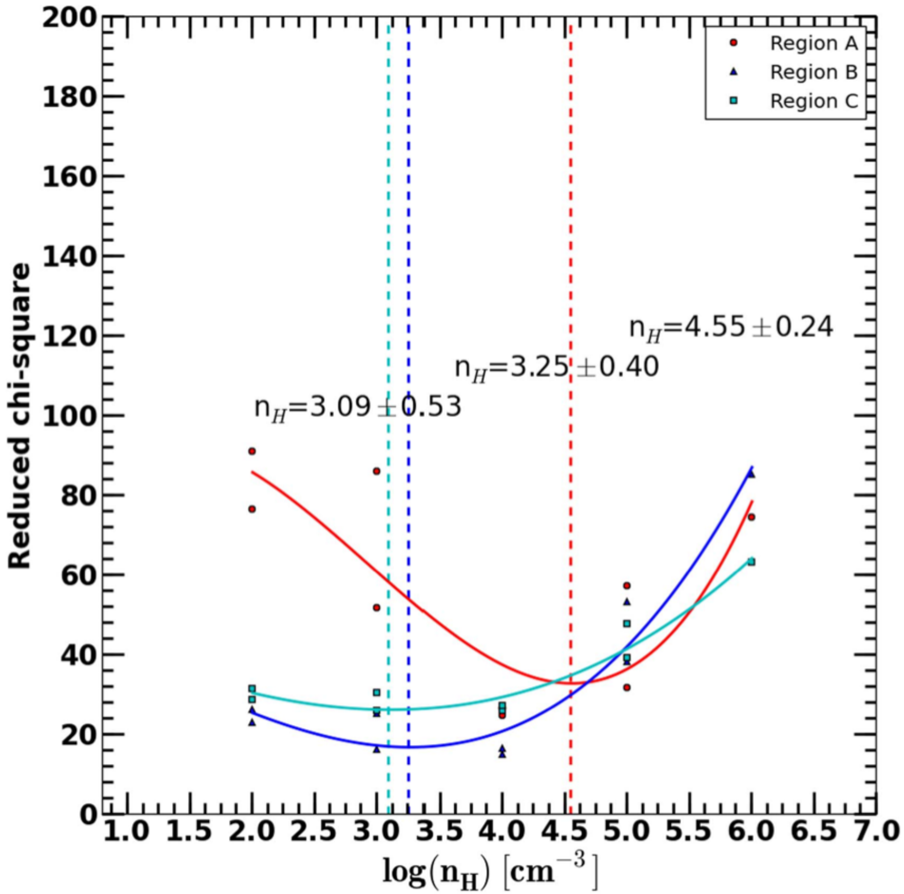

Figure 8. Estimated densities of regions A (red), B (blue), and C (cyan) from DB96. The solid lines display the fitting of reduced chi-squared values of regions A, B, and C. The dashed lines show the minimum reduced chi-squared values from the fitting.

Comparison Data to PDR Model

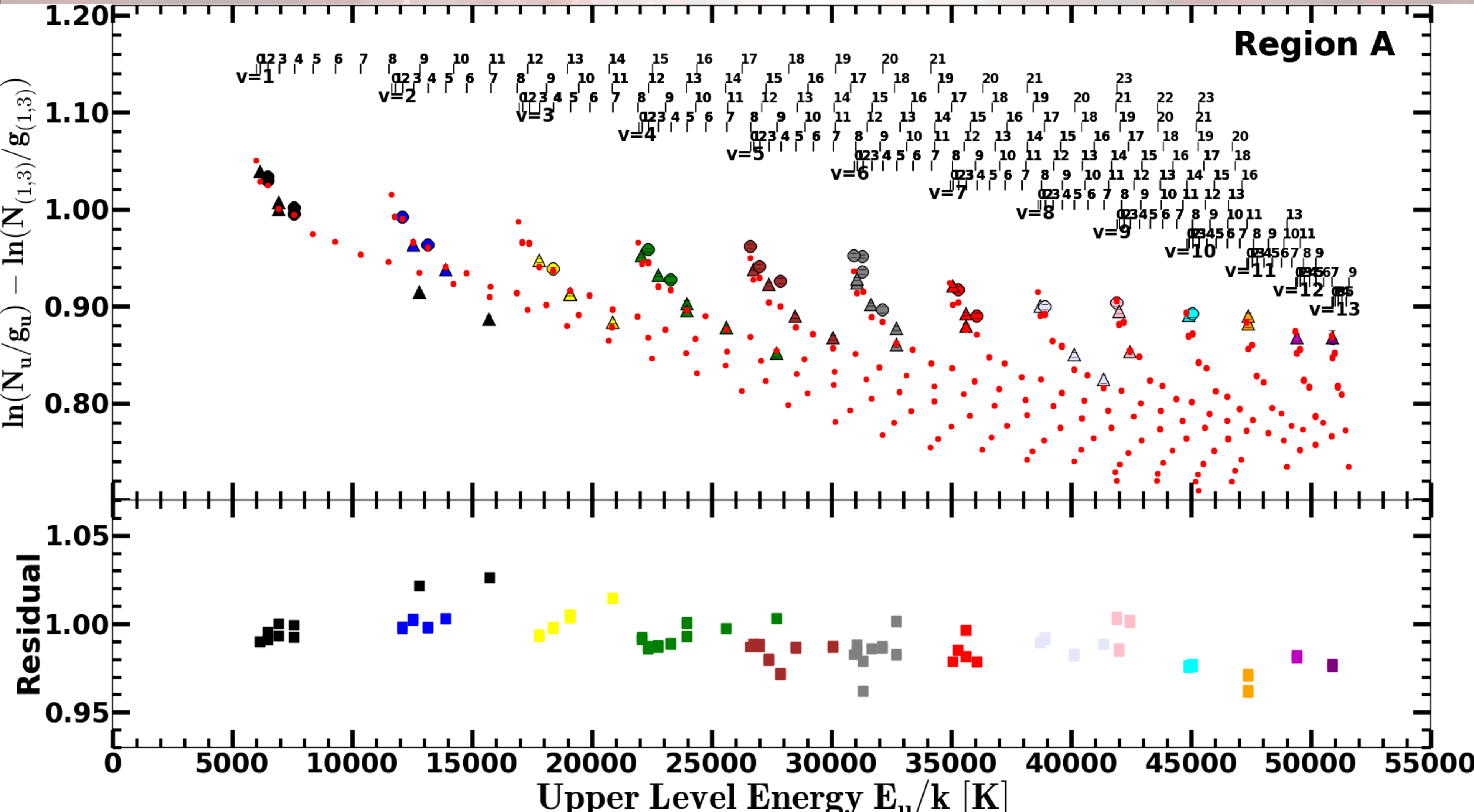

$n\mathrm{H} = 10^5\ \mathrm{cm}^{-3}$ and $G = 10^3\ G^0$

Comparison Data to PDR Model

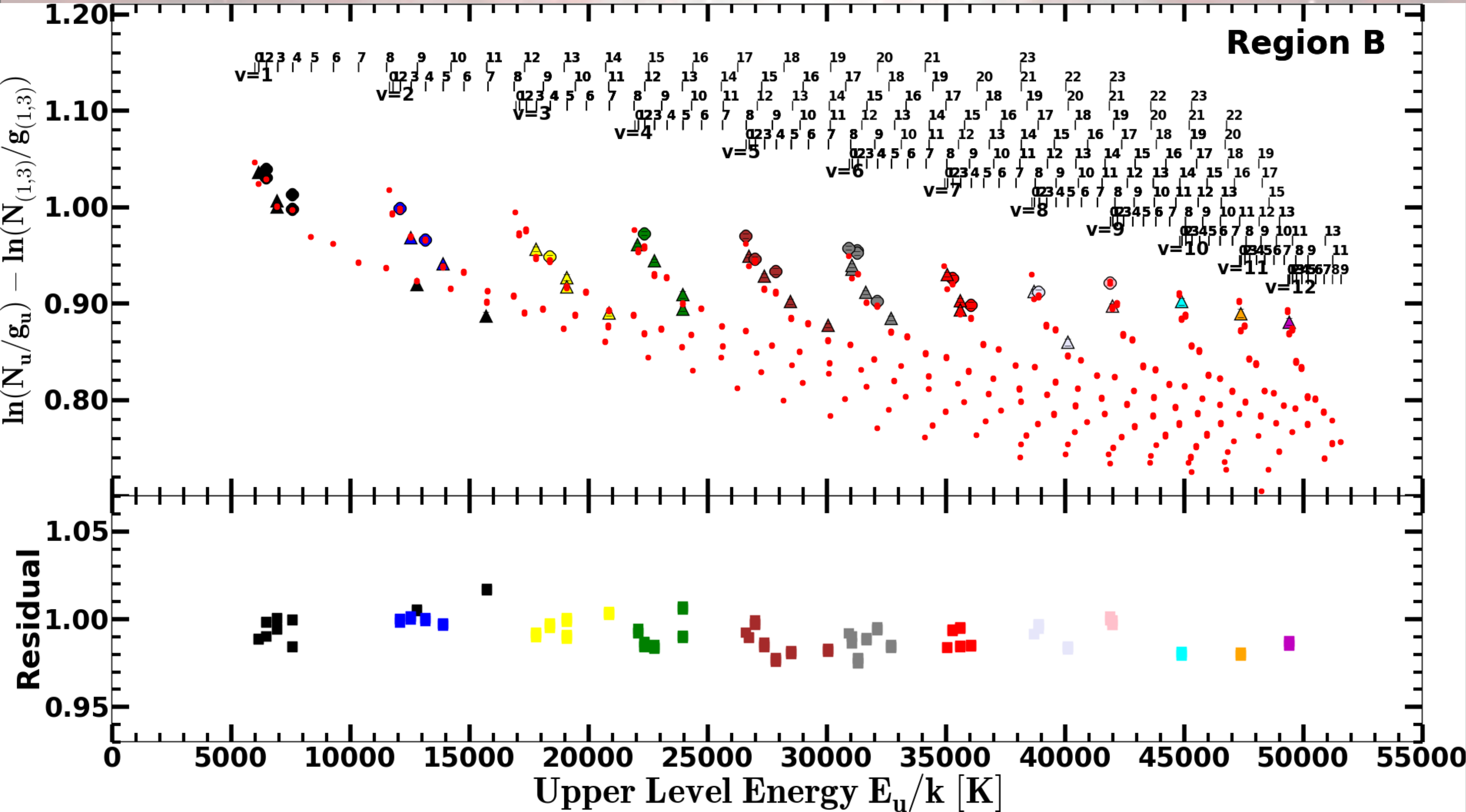

$n\mathrm{H} = 10^4\ \mathrm{cm}^{-3}$ and $G = 10^3\ G^0$.

Comparison Data to PDR Model

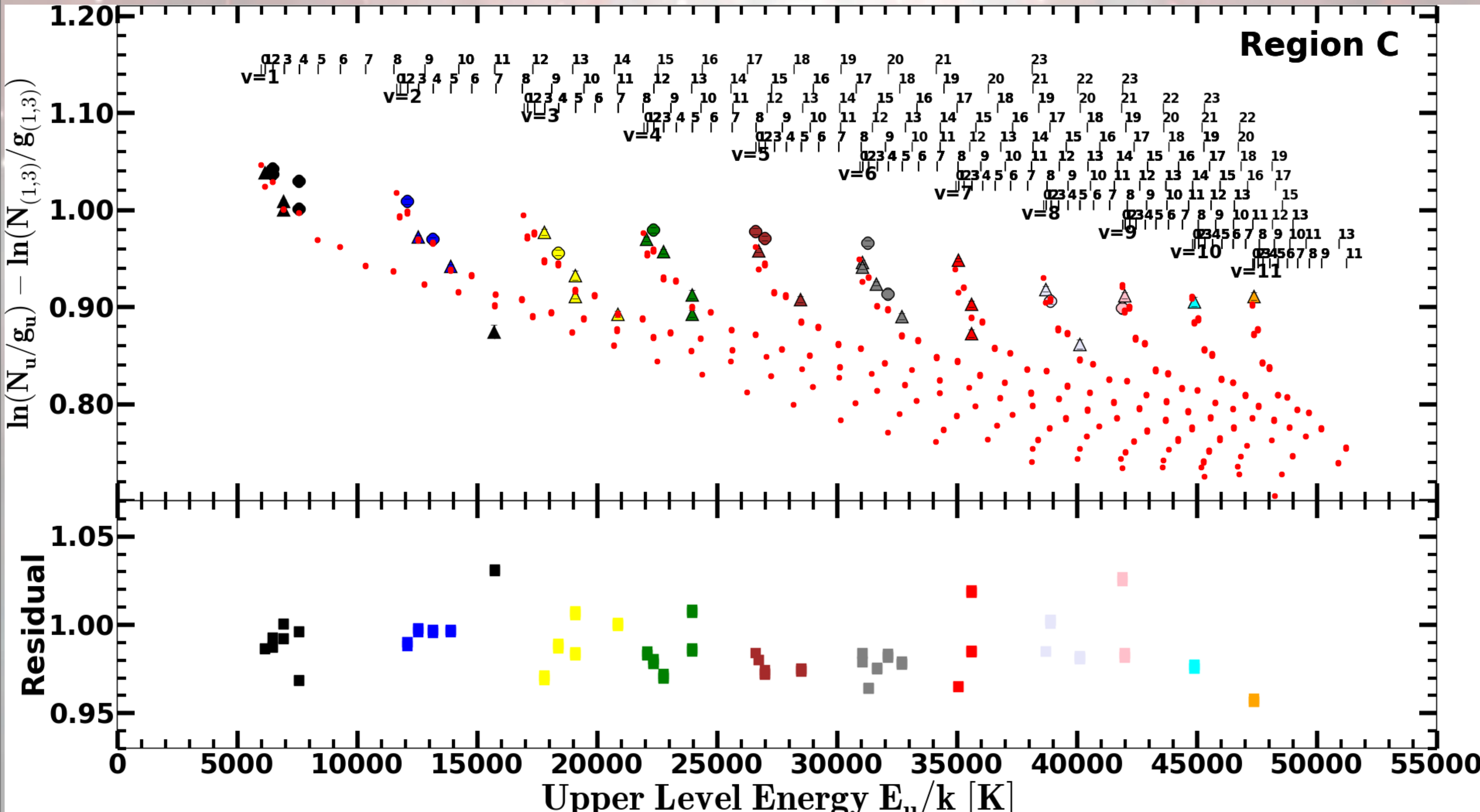

$n\mathrm{H} = 10^4\ \mathrm{cm}^{-3}$ and $G = 10^3\ G^0$.

Derived Densities

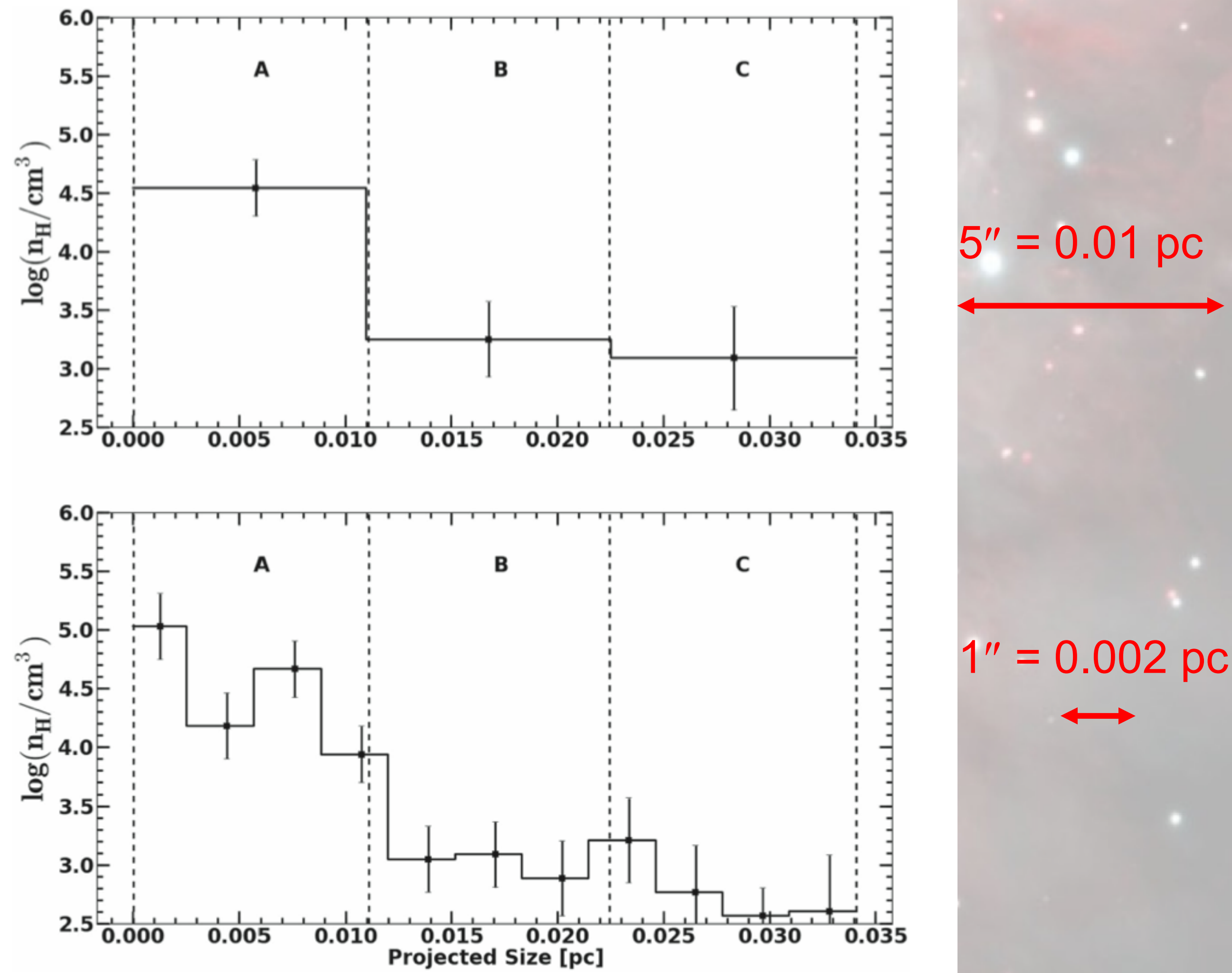

Figure 10. The top plot displays the estimated densities of regions A, B, and C (spatial resolution of ∼5″ or 0.01 pc) from the PDR model of DB96. The solid line shows the estimate densities by DB96. The bottom plot presents the estimated densities of DB96 with a spatial resolution of ∼1″ or 0.002 pc.

Summary and Conclusion

- Detected 68 H_2 ro-vibration lines which are mostly UV excited. Dense regions show collisional de-excitation.
- The presence of the dynamic PDR front relative to the molecular cloud.
- A high density ($n_H \approx 10^5$ cm^{-3}) clumpy structure with a size of ~ 0.002 pc embedded in lower density ($n_H \approx 10^3 - 10^4$ cm^{-3}) regions.

Line ratio (2-1 / 1-0)	OPR	V	ΔV_{FWHM}	n_H
0.41 ± 0.01	1.82 ± 0.11	3.64 ± 0.16	4.63 ± 0.34	10^5
0.48 ± 0.02	1.75 ± 0.09	3.46 ± 0.11	3.29 ± 0.26	10^3-10^4
0.56 ± 0.03	1.63 ± 0.12	3.39 ± 0.22	3.20 ± 0.27	10^3-10^4

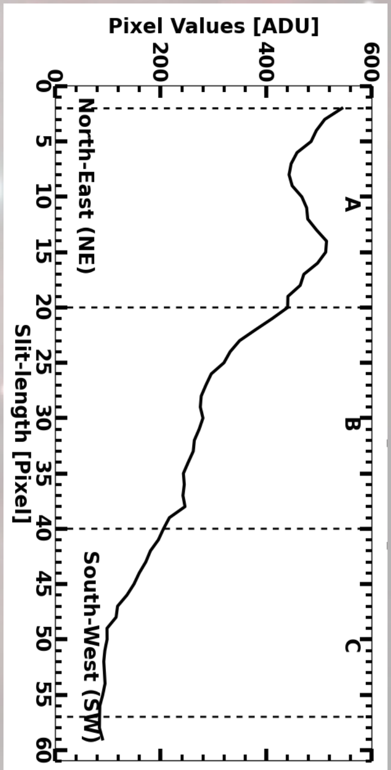

OPR = 2.5 ± 0.3 – position offset 10″ to the north from ours (Martini+1997)

Thank you!

IGRINS information

- Successful commissioning in Gemini South April 2-6.
- Preparing for visiting to Lowell Observatory's Discovery Channel Telescope: September 2018 and April 2019.
- Calls for DCT queue requests and Korean proposals will be sent out in mid-August 2018.
- Contact:
  - Kim Sokal (ksokal@utexas.edu)
  - Greg Mace (gmace@utexas.edu)
  - Hwihyun Kim (hkim@gemini.edu)